INTERNATIONAL JOURNAL FOR NUMERICAL METHODS IN FLUIDS, VOL. 14, 327–341 (1992)

NUMERICAL PREDICTION OF VORTEX SHEDDING BEHIND A SQUARE CYLINDER

KANCHAN M. KELKAR

creare.x Inc., PO Box A-219, Etna Road, Hanover, NH 03755, U.S.A.

AND

SUHAS V. PATANKAR

Department of Mechanical Engineering, University of Minnesota, Minneapolis, MN 55455, U.S.A.

SUMMARY

It is common knowledge that flow around bluff bodies exhibits oscillatory behaviour. The aim of the present study is to compute the steady two-dimensional flow around a square cylinder at different Reynolds numbers and to determine the onset of unsteadiness through a linear stability analysis of the steady flow. Stability of the steady flow to small two-dimensional perturbations is analysed by computing the evolution of these perturbations. An analysis of various time-stepping techniques is carried out to select the most appropriate technique for predicting the growth of the perturbations and hence the stability of the flow. The critical Reynolds number is determined from the growth rate of the perturbations. Computations are then made for periodic unsteady flow at a Reynolds number above the critical value. The predicted Strouhal number agrees well with experimental data. Heat transfer from the cylinder is also studied for the unsteady laminar flow.

KEY WORDS Vortex shedding Unsteady Stability analysis Continuation methods

1. INTRODUCTION

The subject of stability of fluid motion is one of the central problems of fluid mechanics. Occurrence of flow instabilities is commonplace in engineering applications and the importance of the study of such phenomena need not be emphasized. In the present study the focus is on investigating an instability which causes a laminar steady flow behind a square cylinder to give rise to a laminar unsteady flow. The objective is to determine the point of instability using a linear stability analysis of the steady flow.

Stability of fluid motion is a fertile research area and there exists large body of literature on the subject. An attempt is made to summarize the available studies which are directly pertinent to the current investigation. The fundamental ideas of linear stability analysis appear in the texts of Chandrasekhar[1] and Iooss and Joseph.[2] Continuation methods described by Kubicek and Marek[3] have been employed in the present study to compute steady flows. Linear stability has been analysed by solving the initial value problem for the perturbation quantities. Ungar and Brown[4] study the stability of captive rotating drops by computing the eigenvalues of the Jacobians of the corresponding steady flows. A similar approach is utilized by Jenkins and Proctor[5] to determine the flow transitions in Rayleigh–Benard convection. The approach of

0271–2091/92/030327–15$07.50

Received 13 May 1991

solving the initial value problem has been utilized by Ghaddar *et al.*[6,7] in studying the stability of flow over grooved channels. The problem of vortex shedding behind rectangular cylinders has been investigated both numerically and experimentally by Davis *et al.*[8] and Okajima.[9] Gresho and Chan[10] have utilized the problem of unsteady vortex shedding behind a square cylinder as a sample problem for illustrating the use of various discrete projection methods. In all of these studies, computations are limited to the unsteady periodic flow around a rectangular cylinder. A finite element study utilizing linear stability analysis for predicting the onset of vortex shedding behind bluff bodies is presented by Jackson.[11] This study employs solution of the eigenvalue problem for locating the point of instability. In the present study the initial value problem is solved to investigate the linear stability of steady flow around a rectangular cylinder.

The aim of this study is to predict the onset of unsteadiness in the flow around a square cylinder by using linear stability analysis for two dimensions and to compute the periodic vortex shedding at a representative Reynolds number beyond the point of instability. This procedure involves three steps—computation of steady flow at different Reynolds numbers, analysis of linear stability of this flow and subsequent computation of the periodic vortex shedding. This approach, followed by Kelkar,[14] provides a systematic procedure for the investigation of the flow instability and the determination of the onset of unsteadiness. Further, solution of the linearized problem governing the evolution of perturbations to a steady flow is computationally much less intensive than solving the full non-linear unsteady problem for determining the onset of unsteadiness. An analysis of various time-stepping techniques is provided to select a technique which does not modify the nature of the evolution of perturbations and predicts the stability of the steady flow correctly. Details of each of these steps are described in the following sections. Finally, the results of the computations of unsteady laminar heat transfer at a Reynolds number above the critical value are also presented.

2. MATHEMATICAL FORMULATION

The physical problem considered in this study is the two-dimensional flow of an incompressible fluid around a square cylinder placed in a uniform stream. In order to make the problem computationally feasible, artificial confining boundaries are placed around the flow. However, the boundaries are sufficiently far from the body so that their presence has little effect on the characteristics of the flow near the body. Figure 1 shows the computational domain. Since the properties of the fluid are assumed to be constant, the flow field is decoupled from the temperature field. The governing equations and the boundary conditions for the flow and temperature fields are described below.

2.1. *Flow field*

As stated earlier, prediction of the flow field involves computation of the steady flows, their linear stability analysis and computation of the periodic unsteady flows.

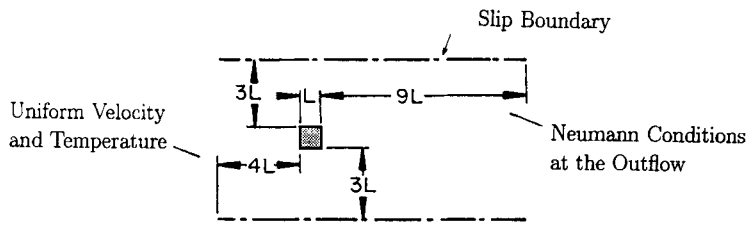

Figure 1. Computational domain for flow around a square cylinder

2.1.1. Steady and unsteady Flow. Steady and unsteady flows are governed by the steady and unsteady forms of the Navier–Stokes equations, respectively. The unsteady, conservative, dimensionless form of these equations in two dimensions for incompressible flow of a constant viscosity fluid is given below:

x-momentum

$$\frac{\partial U}{\partial \tau}+\frac{\partial (UU)}{\partial X}+\frac{\partial (VU)}{\partial Y}=-\frac{\partial P}{\partial X}+\frac{1}{Re}\left(\frac{\partial^2 U}{\partial X^2}+\frac{\partial^2 U}{\partial Y^2}\right), \tag{1}$$

y-momentum

$$\frac{\partial V}{\partial \tau}+\frac{\partial (UV)}{\partial X}+\frac{\partial (VV)}{\partial Y}=-\frac{\partial P}{\partial Y}+\frac{1}{Re}\left(\frac{\partial^2 V}{\partial X^2}+\frac{\partial^2 V}{\partial Y^2}\right), \tag{2}$$

continuity

$$\frac{\partial U}{\partial X}+\frac{\partial V}{\partial Y}=0, \tag{3}$$

with

$$U=\frac{u}{u_\infty}, \qquad V=\frac{v}{u_\infty}, \qquad \tau=\frac{tu_\infty}{L}, \qquad X=\frac{x}{L}, \qquad Y=\frac{y}{L}, \qquad P=\frac{p}{\rho u_\infty^2}. \tag{4}$$

Here u_∞ is the uniform velocity of the fluid far away from the body. The boundary conditions are as follows:

left boundary

$$U=1, \qquad V=0, \tag{5a}$$

right boundary

$$\frac{\partial U}{\partial X}=0, \qquad \frac{\partial V}{\partial X}=0, \tag{5b}$$

top and bottom boundaries

$$\frac{\partial U}{\partial Y}=0, \qquad V=0, \tag{5c}$$

solid surface of the cylinder

$$U=0, \qquad V=0. \tag{5d}$$

The only governing parameter for this problem is the Reynolds number based on the length L of the sides of the square cylinder and is defined as

$$Re=\frac{\rho u_\infty L}{\mu}. \tag{6}$$

The steady flow field is governed by the same set of equations devoid of the unsteady term $\partial/\partial\tau$.

2.1.2. Linear stability analysis. This analysis involves the assumption that the perturbations to the steady flow are infinitesimally small. In the present study the stability of the two-dimensional

steady flow is analysed with respect to two-dimensional perturbations. Thus, in carrying out a linear stability analysis, all higher-order terms in perturbation quantities are neglected. Suppose that linear stability of a steady flow denoted by (U_S, V_S, P_S) is being analysed. Then the governing equations for the two-dimensional perturbation quantities (U', V', P') are obtained by linearizing the unsteady Navier–Stokes equations about the steady base flow. The boundary conditions for the perturbations are obtained by applying the boundary conditions of equation (5) to the total velocity ($U+U'$, $V+V'$). The resulting dimensionless equations and the boundary conditions are described below:

u-perturbation

$$\frac{\partial U'}{\partial \tau}+\frac{\partial (U_S U')}{\partial X}+\frac{\partial (V_S U')}{\partial Y}=-\frac{\partial P'}{\partial X}+\frac{1}{Re}\left(\frac{\partial^2 U'}{\partial X^2}+\frac{\partial^2 U'}{\partial Y^2}\right)-U'\frac{\partial U_S}{\partial X}-V'\frac{\partial U_S}{\partial Y}, \tag{7}$$

v-perturbation

$$\frac{\partial V'}{\partial \tau}+\frac{\partial (U_S V')}{\partial X}+\frac{\partial (V_S V')}{\partial Y}=-\frac{\partial P'}{\partial Y}+\frac{1}{Re}\left(\frac{\partial^2 V'}{\partial X^2}+\frac{\partial^2 V'}{\partial Y^2}\right)-U'\frac{\partial V_S}{\partial X}-V'\frac{\partial V_S}{\partial Y}, \tag{8}$$

continuity

$$\frac{\partial U'}{\partial X}+\frac{\partial V'}{\partial Y}=0. \tag{9}$$

Note that, in deriving the above set of equations, use is made of the fact that the base flow (U_S, V_S, P_S) satisfies the steady equations. The quantities U', V' and P' are dimensionless perturbation velocities and pressures and are non-dimensionalized in the same manner as in equation (5). The boundary conditions for the perturbation quantities are as follows:

left boundary

$$U'=0, \qquad V'=0, \tag{10a}$$

right boundary

$$\frac{\partial U'}{\partial X}=0, \qquad \frac{\partial V'}{\partial X}=0, \tag{10b}$$

top and bottom boundaries

$$\frac{\partial U'}{\partial Y}=0, \qquad V'=0, \tag{10c}$$

solid surface of the cylinder

$$U'=0, \qquad V'=0. \tag{10d}$$

Then, in assessing the linear stability of a given steady flow (U_S, V_S, P_S), the evolution of the perturbations, starting from an entirely arbitrary initial perturbation, is evaluated. If for all possible initial perturbations the perturbations decay, the flow is linearly stable. If, however, there exists at least one initial condition for which the perturbations grow, the flow is termed linearly unstable.

2.1.3. Temperature field. Since the properties of the fluid are constant, the temperature field needs to be computed only after a converged velocity field is obtained. For each steady and unsteady flow field the corresponding temperature field is computed by solving the energy equation. The square cylinder is assumed to be isothermally heated, exchanging heat to the cold fluid flowing around it, which is at a uniform temperature T_∞ far away from the cylinder. The unsteady dimensionless form of the governing equation (assuming negligible viscous dissipation) and the corresponding boundary conditions are given below:

$$\frac{\partial\theta}{\partial\tau}+\frac{\partial(U\theta)}{\partial X}+\frac{\partial(V\theta)}{\partial Y}=\frac{1}{Pr}\left(\frac{\partial^2\theta}{\partial X^2}+\frac{\partial^2\theta}{\partial Y^2}\right), \tag{11}$$

with

$$\theta=\frac{T-T_\infty}{T_W-T_\infty}, \qquad Pr=\frac{\mu Cp}{K}. \tag{12}$$

Here T_∞ is the uniform temperature of the fluid far away from the body and T_W is the temperature at which the square cylinder is maintained. Then, the boundary conditions for the temperature field are as follows:

left boundary

$$\theta=0, \tag{13a}$$

right boundary

$$\frac{\partial\theta}{\partial X}=0, \tag{13b}$$

top and bottom boundaries

$$\frac{\partial\theta}{\partial Y}=0, \tag{13c}$$

solid surface of the cylinder

$$\theta=1. \tag{13d}$$

The governing parameter for the temperature field is the Prandtl number of the fluid, Pr, in addition to the Reynolds number which governs the velocity field. In the present study all the computations for the temperature field are made for $Pr=0{\cdot}7$. The steady temperature field for a given velocity field is governed by equation (11) devoid of the unsteady term. Note that the temperature field does not enter the linear stability analysis because the velocity field is decoupled from the temperature field owing to the assumption of constant fluid properties.

3. SOLUTION METHOD

The governing equations described above are discretized on a Cartesian grid and the resulting set of algebraic equations is solved to obtain a discrete solution of the problem. The details of the discretization, the strategies employed for obtaining steady solutions, the stability analysis and the techniques used for the solution of the algebraic equations are now described.

3.1. Discretization method

The discretization method used in the present study utilizes a control volume formulation. The domain of interest is divided into a set of discrete control volumes. A grid point is located at the centre of each control volume and the value of the conserved variable is stored at each of the grid points. Discretization equations for the nodal unknown at a grid point are then obtained by conserving the flux of that variable over the control volume that surrounds the grid point. This requires the evaluation of the total flux of the conserved variable through each face of the control volume. In the present study the power-law scheme proposed by Patankar[12] is used to compute the combined convection and diffusion flux through a control volume face in terms of the values of the variable at the grid points which envelop the face. A staggered grid is employed for storing the velocity components. Thus the control volume for the x- (or y-) direction velocity is displaced in the x- (or y-) direction with respect to the control volume for continuity. This use of a staggered grid prevents the occurrence of checkerboard pressure fields. A detailed description of this discretization method is given by Patankar.[12]

3.2. Computation of steady flows using continuation

The first step in the analysis is to obtain steady flows at different Reynolds numbers. If the steady flow being sought is unstable, iterative solution techniques such as SIMPLER,[12] which solve discretized momentum and continuity equations in a segregated manner, are unlikely to converge to a solution when utilized for solving the steady form of the discretized equations. Alternative techniques that incorporate direct matrix solution of the discretization equations with a good starting guess to the solution are needed to compute the steady flow. Continuation methods can be used to construct a good initial guess.

Any of the continuation methods described by Kubicek and Marek[3] provides a systematic way for computing steady flows. Since in this problem the solution branch for steady solutions at different Reynolds numbers is expected to be monotonic, a Newtonian–Raphson continuation, instead of a more complicated arc length continuation, is sufficient and has been employed in the present study. The details of the Newton–Raphson continuation procedure are described here.

The set of algebraic discretization equations for steady flow can be written as

$$\mathbf{AZ} = \mathbf{B} \tag{14}$$

or more conveniently as

$$\mathbf{F}(\mathbf{Z}, Re) = 0, \tag{15}$$

where the vector of nodal unknowns, $\mathbf{Z}$, is

$$\mathbf{Z} \equiv (\mathbf{U}, \mathbf{V}, \mathbf{P}). \tag{16}$$

This continuation procedure, in essence, consists of starting from a known solution and extrapolating along the local tangent to the solution branch to obtain an initial guess to the solution at the desired increment in the value of the parameter and then iteratively refining this initial guess to obtain the exact solution at this new value of the parameter. Mathematically, this is equivalent to expanding the left side of equation (15) as a Taylor series around the starting solution $(\mathbf{Z}_0, Re_0)$ and neglecting all higher-order terms. Thus

$$\mathbf{J}_0 \Delta \mathbf{Z} + \left(\frac{\partial \mathbf{F}}{\partial Re} \right)_{(\mathbf{Z}_0, Re_0)} \Delta Re = 0, \tag{17}$$

where $\mathbf{J}_0$ denotes the Jacobian matrix at $\mathbf{Z}_0$. Thus starting from $(\mathbf{Z}_0, Re_0)$, for a given ΔRe, an

initial guess $\mathbf{Z}^* = \mathbf{Z}_0 + \Delta\mathbf{Z}$ can be constructed for the solution at $Re = Re_0 + \Delta Re$. This initial guess is improved using a Newton–Raphson iteration to obtain the correct solution at Re as

$$\mathbf{J}^n \Delta\mathbf{Z}^{n+1} = -\mathbf{F}(\mathbf{Z}^n, Re) \tag{18}$$

and

$$\mathbf{Z}^{n+1} = \mathbf{Z}^n + \Delta\mathbf{Z}^{n+1} \tag{19}$$

until $\Delta\mathbf{Z}^n$ is small. Here n indicates the number of iterations of the Newton–Raphson procedure. Note that equations (18) and (19) represent an iteration of the Newton–Raphson procedure performed to obtain the correct solution at $Re_0 + Re$ and are distinct from the first-order continuation represented by equation (17).

If the increment ΔRe in extrapolating the solution as in equation (17) is not large, the initial guess $\mathbf{Z}^*$ is very close to the correct solution and subsequent Newton–Raphson iterations converge rapidly. Thus, starting from a known solution $(\mathbf{Z}_0, Re_0)$, by solving equation (17) in conjunction with equations (18) and (19), the steady solutions can be computed at the desired increments in Reynolds number.

3.3. Linear stability analysis

3.3.1. Initial value problem. To analyse the linear stability of a computed steady flow, the corresponding discrete equations governing the evolution of small perturbations to this steady flow are required. Analogous to the derivation of equations (7) and (8) from equations (1) and (2), discrete equations for the evolution of the perturbation are obtained directly by linearizing the discretization equations around the steady flow solution, the stability of which is to be analysed. Thus let the steady flow, the stability of which is to be investigated, be denoted by $(\mathbf{Z}_S, Re_S)$. Then the small perturbations to this flow are governed by

$$\mathbf{M}\frac{d\mathbf{Z}'}{d\tau} + \mathbf{J}_S\mathbf{Z}' = 0, \tag{20}$$

where $\mathbf{Z}' \equiv (\mathbf{U}', \mathbf{V}', \mathbf{P}')$ are discrete perturbations and $\mathbf{J}_S$ is the Jacobian matrix evaluated at the steady solution. Since the flow is assumed to be incompressible, the unsteady term in the continuity equation is absent. Hence the matrix $\mathbf{M}$ in the above equation has unit values along the part of the diagonal that corresponds to the unsteady term in the linearized momentum equations and contains zeros everywhere else. This set of equations needs to be solved for arbitrary initial conditions on the perturbations. Note that equation (20) can also be solved as an eigenvalue problem. Then the real part of the most unstable eigenvalue indicates whether the flow is stable or unstable and the corresponding eigenvector gives the most unstable form of the perturbation. In the present study equation (20) is solved as an initial value problem, because the interest lies in determining the stability of the flow and hence only in the most unstable eigenvalue, and the solution of the initial value problem asymptotically filters out this most unstable eigenvalue and the corresponding most unstable form of the perturbation to the steady flow. The initial condition on perturbations is chosen to be an arbitrary asymmetric variation of grid point excitations. Analogous to the observation that a particular harmonic is unlikely to be absent in the Fourier spectrum of an arbitrary waveform, it is virtually unlikely that the most dangerous perturbation (most unstable eigenfunction) will escape an arbitrary asymmetric variation of initial perturbations. Then, by choosing an appropriate temporal discretization, the evolution of perturbations can be computed starting from an initial guess. If the perturbations decay asymptotically, the steady flow is linearly stable, while if the perturbations grow, the flow is

unstable. By studying the variation of the asymptotic rate of growth of perturbations to the steady flow with Reynolds number, the point of instability can be determined.

3.3.2. Choice of time-stepping scheme. The asymptotic behaviour of perturbations computed by solving an initial value problem is subject to errors introduced by temporal discretization. Therefore the temporal discretization scheme should be properly selected to predict the point of instability of the steady flow. An analysis of implicit, explicit and Crank–Nicholson time-stepping techniques is carried out to demonstrate the suitability of the Crank–Nicholson technique.

Consider a model linear initial value problem as follows:

$$\frac{d\mathbf{R}}{dt}=\mathbf{G}\mathbf{R} \tag{21}$$

subject to an initial condition on **R**. This model problem is chosen over the original problem described by equation (20) in order to elucidate the analysis of time-stepping techniques and to isolate this analysis from the apparent complication of the absence of the unsteady term in the continuity equations for grid point perturbations which is addressed later in this section. Let an eigenvalue of matrix **G** be denoted by σ. Then the evolution of the magnitude $C(t)$ of the corresponding eigenvector from its initial magnitude $C(0)$ is given by

$$\frac{dC(t)}{dt}=\sigma C(t), \tag{22}$$

where $\sigma=\sigma_r+i\sigma_i$.

Although the following analysis applies to any eigenvalue for the matrix **G**, in the context of stability analysis it is taken to be the most unstable eigenvalue of the matrix **G**. Then temporal discretization yields

$$\frac{C^{n+1}-C^n}{\Delta t}=\sigma[\alpha C^{n+1}+(1-\alpha)C^n], \tag{23}$$

where C^n denotes the value of C at time level n and α is a fraction such that $\alpha=0$, 1 and 0·5 correspond to explicit, implicit and Crank–Nicholson time stepping respectively. Then the amplification of $C(t)$ for a time step is defined as

$$f=\frac{C^{n+1}}{C^n}=\frac{1+(1-\alpha)\sigma\Delta t}{1-\alpha\sigma\Delta t}. \tag{24}$$

Note that for a finite time step size the amplification factor will always be in error from the analytical value of $e^{\sigma\Delta t}$. However, in order to locate the point of instability correctly, the desirable time stepping should predict a growth (decay) of $C(t)$ if the real part σ_r of the eigenvalue σ is positive (negative), i.e.

$$\begin{aligned} |f|^2-1>0 \quad &\text{when } \sigma_r>0,\\ |f|^2-1<0 \quad &\text{when } \sigma_r<0,\\ |f|^2-1=0 \quad &\text{when } \sigma_r=0. \end{aligned} \tag{25}$$

For explicit time stepping, equation (24) with $\alpha=0$ yields

$$|f|^2-1=2\sigma_r\Delta t+(\sigma_r^2+\sigma_i^2)\Delta t^2. \tag{26}$$

Thus, clearly, the explicit time stepping introduces an additional growth of perturbations at $\sigma_r=0$ and can result in an underprediction of the point of instability.

For implicit time stepping ($\alpha = 1$)

$$|f|^2 - 1 = \frac{1}{1 - 2\sigma_r \Delta t + (\sigma_r^2 + \sigma_i^2)\Delta t^2}. \tag{27}$$

Thus the implicit time stepping introduces an extra decay of perturbations at $\sigma_r = 0$ and can result in overprediction of the point of instability.

For Crank–Nicholson time stepping ($\alpha = 0{\cdot}5$)

$$|f|^2 - 1 = \frac{2\sigma_r \Delta t}{(1 - 0{\cdot}5\sigma_r \Delta t)^2 + (0{\cdot}5\sigma_i \Delta t)^2}. \tag{28}$$

Thus the Crank–Nicholson technique obeys the conditions in equation (25). Therefore, if this technique is used to compute the evolution of perturbations, they will always decay (grow) when the flow is stable (unstable), though at a rate which is of second-order accuracy compared to the analytical value.

Note that the linear stability problem described by equation (20) can be reduced to the form of equation (21) by Gaussian elimination of unknown perturbation pressures, so that the results of this analysis are equally applicable to temporal discretization for the problem of interest. Hence the Crank–Nicholson time-stepping technique is adopted for calculation of the evolution of perturbations to the steady flow. Owing to the second-order accuracy of the Crank–Nicholson scheme, it is also employed for the computation of the periodic flow that occurs after the onset of instability.

3.4. Computational details

A rectangular grid of size 80×80 is employed for discretization. The grid is finer near the surfaces of the square cylinder to better resolve the gradients near the wall. A computation of steady flow for $Re = 50$ with a grid of 120×120 changed the drag coefficient on the body by 0·85%. As stated earlier, the boundaries of the domain are located sufficiently far from the body so as not to affect the flow near the body. The particular distances are shown in Figure 1. Any further movement of these boundaries away from the body changed the drag coefficient for steady flow around the body at $Re = 50$ by only 0·54% for a grid of 80×80. Hence this grid size is deemed sufficiently fine for accurate computations.

The continuation procedure described earlier is used to compute steady flow at Reynolds numbers between 10 and 100 at fixed increments of 10 with a known starting solution at $Re = 0{\cdot}1$. Linear stability of each of the computed steady flows is studied by solving the initial value problem for the perturbation quantities and the critical Reynolds number (point of instability) is determined. A variety of initial guesses for perturbations were used for the case of $Re = 70$ to ensure that the asymptotic form and growth rate of perturbations are independent of the arbitrarily chosen initial perturbations and that, in general, an arbitrarily chosen initial condition on perturbation is very unlikely to exclude the most unstable form of perturbations. Finally, periodic unsteady flow is computed at $Re = 100$, which is above the point of instability. A dimensionless time step of 0·12 is used for unsteady computations of perturbations as well as the unsteady periodic flow to resolve the unsteady behaviour accurately.

Direct as well as iterative solution techniques are used for solving the algebraic equations. Direct matrix solution is used for systems of equations which arise in Newton–Raphson continuation (equations (17) and (18)) for reasons described earlier and in the calculation of the evolution of perturbations (equation (20)) for linear stability analysis of steady flow as well. It is worth noting that the direct solution technique is particularly suited for the solution of the linear

stability problem because the problem is linear and for a fixed value of the time step the coefficient matrix is fixed so that it can be factorized once at the start of the calculation. The Yale Sparse Matrix Package by Eisenstat *et al.*[13] is used for direct solution of the algebraic equations. The iterative solution procedure SIMPLER, proposed by Patankar,[12] is employed for the computation of the unsteady flow at $Re = 100$ as well as for constructing a starting solution of steady flow at $Re = 0{\cdot}1$ for the continuation procedure.

4. RESULTS AND DISCUSSION

Results of the steady flow computations, their stability analysis and subsequent computation of the periodic flow at a Reynolds number above the limit of stability will now be described.

4.1. Steady flow and linear stability analysis

Figure 2 shows streamline patterns for some of the computed two-dimensional steady flows. As the Reynolds number increases, the size and strength of the recirculation increase. The evolution of small two-dimensional perturbations to these steady flows is obtained from the stability analysis. Figure 3 shows the evolution of u-velocity perturbations at two points in the vicinity of the square cylinder—one upstream (position 1) and one downstream (position 2) of the square cylinder—for $Re = 50$ and 60. Note that for $Re = 50$ all the perturbations decay asymptotically while for $Re = 60$ the perturbations grow with time. Thus the point of instability lies between $Re = 50$ and 60. To obtain the critical Reynolds number more accurately, the variation of the real part of the dimensionless growth rate of the perturbations with Reynolds number is plotted in Figure 4. The critical Reynolds number then corresponds to $\sigma_r = 0$ and is seen to have a value of 53. Thus a steady flow cannot persist beyond this Reynolds number and is not expected to be observed in practice. Figure 5 shows the form of instantaneous streamlines of the most unstable perturbation for $Re = 50$ and 60. The two-dimensional unsteady flow after the critical Reynolds number results from an interaction of this unstable perturbation and the original unstable steady flow. Also, since the perturbations evolve in an oscillatory manner as seen in Figure 3, the flow

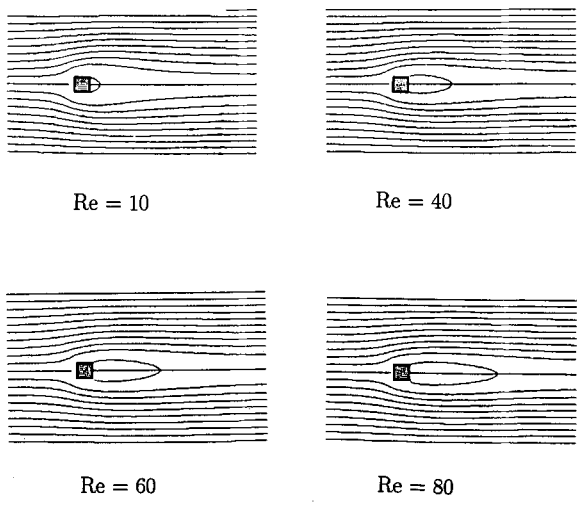

Figure 2. Streamline patterns for steady flow around a square cylinder at different Reynolds numbers

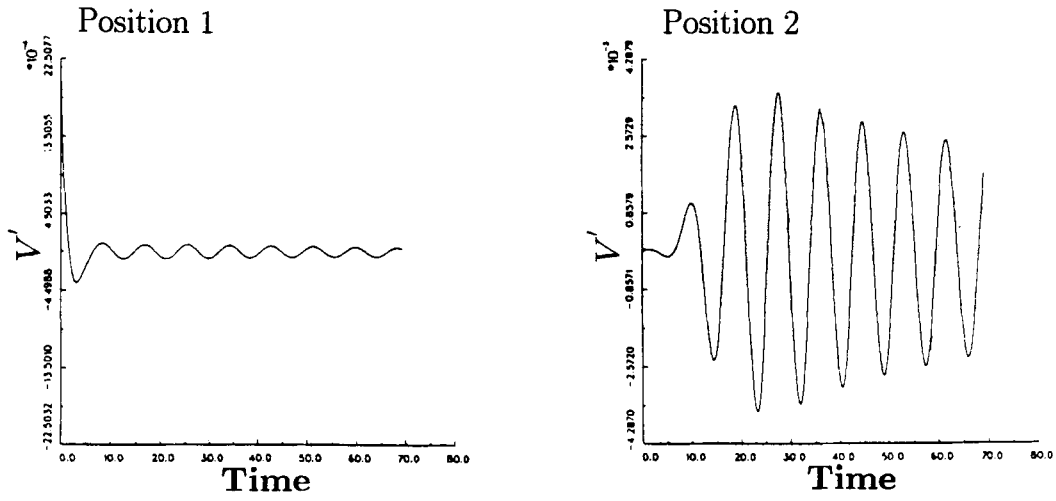

Re = 50

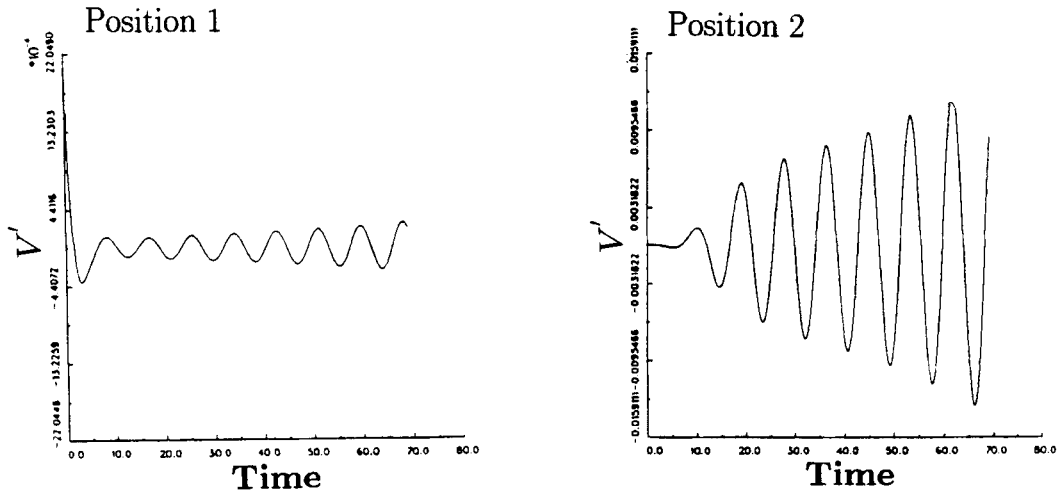

Re = 60

Figure 3. Variation of small perturbations with dimensionless time at two positions in the vicinity of a square cylinder at $Re = 50$ and 60

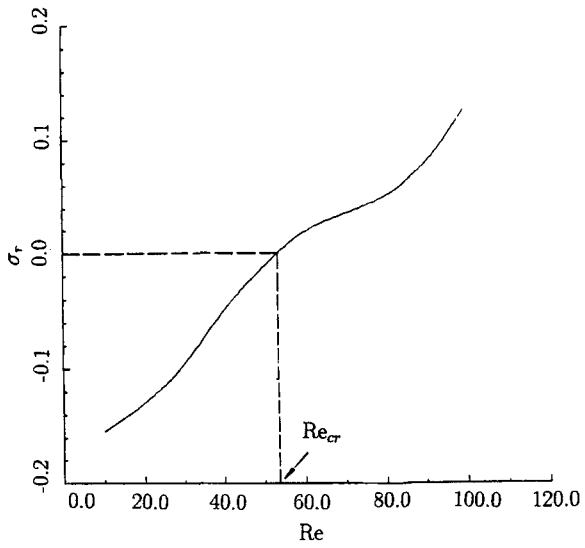

Figure 4. Variation of the growth rate of the most unstable perturbation to the steady flow with Reynolds number

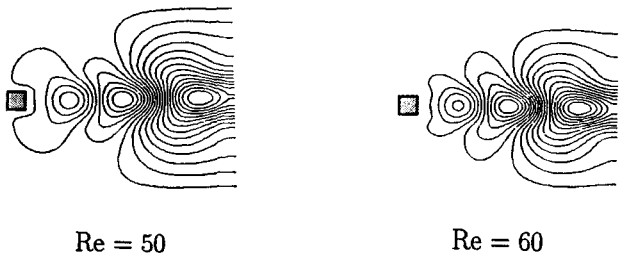

Figure 5. Instantaneous streamlines of the most unstable perturbation to the steady flow at $Re = 50$ and 60

after the critical point is unsteady and time-periodic and the bifurcation at the point of instability is a Hopf bifurcation.

Some comments on the involved computational costs are in order. Computations were carried out on a CYBER-205 supercomputer. The computation of the unsteady flow at $Re = 100$ required 3·7 CPU hours for the seven periodic cycles and the initial transient appearing in Figure 8, while solution of a typical initial value problem for the evolution of perturbations to a steady flow, the stability of which is to be determined, required 0·85 CPU hours for the same number of time steps.

4.2. Unsteady flow

The periodic vortex shedding obtained after the critical Reynolds number has been computed at $Re = 100$. Streamlines for the unstable steady flow at this Reynolds number are shown in Figure 6. Figure 7 shows instantaneous streamlines and isotherms at three different times within a cycle of the periodic vortex shedding (starting and ending instants are the same). The oscillatory nature of the wake behind the cylinder can be clearly seen in these patterns.

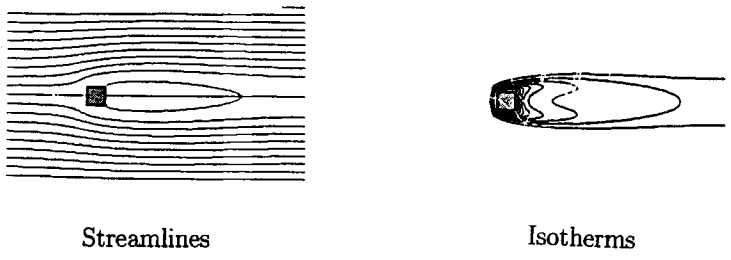

Figure 6. Streamlines and isotherm pattern for unstable steady flow at $Re = 100$ and $Pr = 0{\cdot}7$

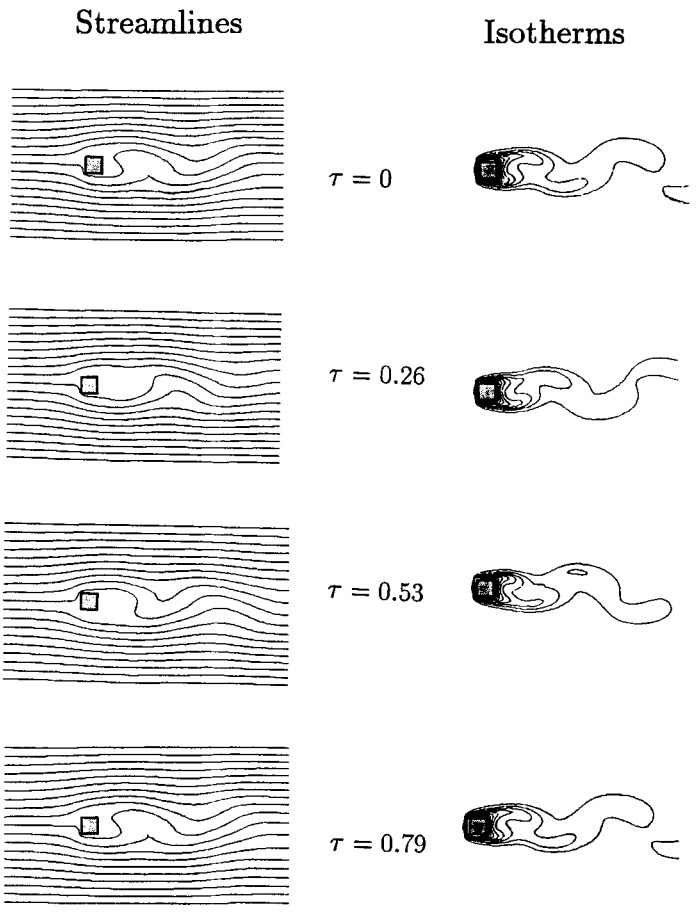

Figure 7. Instantaneous streamlines and isotherm patterns during one cycle of periodic unsteady flow behind a square cylinder at $Re = 100$ with $Pr = 0{\cdot}7$

Figure 8 shows the variation of the lift and drag coefficients for the cylinder, defined as $C_L = F_L/(\frac{1}{2}\rho U_\infty^2 L)$ and $C_D = F_D/(\frac{1}{2}\rho U_\infty^2 L)$, F_L and F_D being the lift and drag forces on the cylinder. The period of oscillation of the lift coefficient gives a Strouhal number of 0·126, which agrees very well with the experimental value of 0·118 reported by Okajima.[9] The overall Nusselt number for the body, however, does not show much oscillation, as seen in Figure 9, owing to the averaging effect of the oscillating wake. The value of the Nusselt number is 3·25 compared to the value of 3·298 for the steady flow, indicating that the unsteady flow does not augment heat transfer from the cylinder in any significant manner. However, the temperature fields in the wake

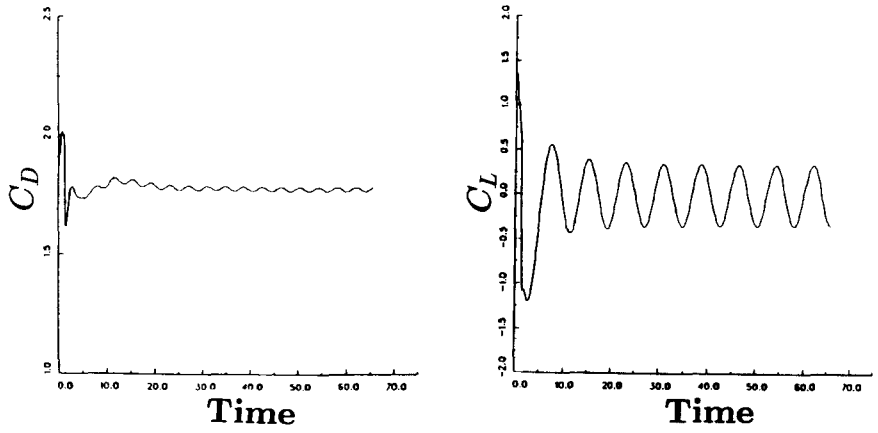

Figure 8. Variation of lift and drag coefficients for a square cylinder with time for unsteady flow at $Re = 100$

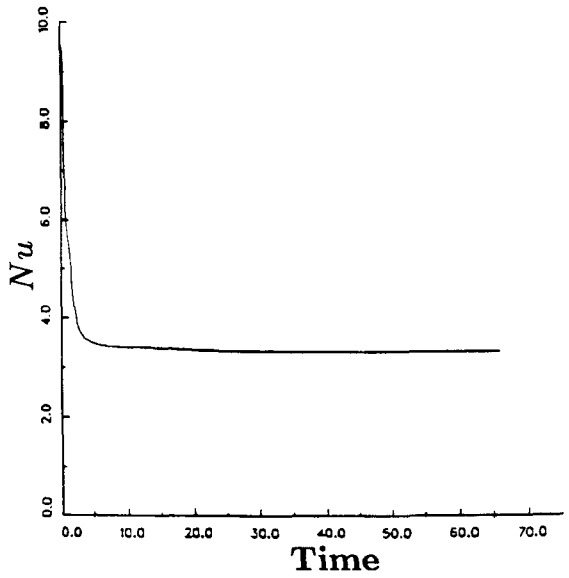

Figure 9. Variation of the Nusselt number for a square cylinder with time for unsteady flow at $Re = 100$

for steady and unsteady flow at $Re = 100$ are entirely different, as seen from a comparison of the isotherm patterns in Figures 6 and 7.

5. CONCLUSIONS

Linear stability analysis is used to predict the onset of instability in the flow around a square cylinder. The two-dimensional steady flow around the cylinder at different Reynolds numbers is computed using the Newton–Raphson continuation technique. The stability of these steady flows to small two-dimensional disturbances is analysed by solving the initial value problem for the perturbation quantities. An analysis of the time-stepping techniques shows that the Crank–Nicholson technique, irrespective of the size of time step used, predicts the temporal behaviour of the perturbations and hence the stability of the steady flow correctly. The critical Reynolds number is inferred from the variation of the rate of growth of the perturbations with the Reynolds number. Computations for unsteady flow at a Reynolds number above the critical value yield a value of the Strouhal number which is very close to its experimentally observed value. Finally, although the temperature fields in the wake for steady and unsteady flow are quite different, the overall heat tfansfer from the square cylinder in unsteady flow is almost the same as that in steady flow.

ACKNOWLEDGEMENT

The support of the Minnesota Supercomputer Institute for the present work is gratefully acknowledged.

REFERENCES

1. S. Chandrasekhar, *Hydrodynamic and Hydromagnetic Stability*, Dover, New York, 1961.
2. G. Iooss and D. D. Joseph, *Elementary Stability and Bifurcation Theory, Undergraduate Texts in Mathematics*, Springer, New York, 1980.
3. M. Kubicek and I. Marek, *Computational Methods in Bifurcation Theory and Dissipative Structures*, Springer, New York, 1983.
4. L. H. Ungar, R. A. Brown, 'The dependence of the shape and stability of captive rotating fluid drops on multiple parameters', *Phil. Trans. R. Soc. Lond. A*, **306**, 347–370 (1982).
5. D. R. Jenkins and M. R. E. Proctor, 'The transition from roll to square cell pattern in Rayleigh–Bernard convection', *J. Fluid Mech.*, **139**, 461–471 (1984).
6. N. K. Ghaddar, K. Z. Korczak, B. B. Mikic and A. T. Patera, 'Numerical investigation of incompressible flow in grooved channels, Part 1: Stability and self sustained oscillations', *J. Fluid Mech.*, **168**, 541–567 (1986).
7. N. K. Ghaddar, K. Z. Korczak, B. B. Mikic and A. T. Patera, 'Numerical investigation of incompressible flow in grooved channels, Part 2: Resonance and oscillatory heat-transfer enhancement', *J. Fluid Mech.*, **168**, 541–567 (1986).
8. R. W. Davis, E. F. Moore and L. P. Purtell, 'A numerical and experimental study of confined flow around rectangular cylinders', *Phys. Fluids*, **27**, 46–59 (1984).
9. A. Okajima, 'Strouhal numbers for rectangular cylinders', *J. Fluid Mech.*, **123**, 379–398 (1982).
10. P. M. Gresho and S. T. Chan, 'On the theory of semi-implicit projection methods for viscous incompressible flow and its implementation via a finite element method that also introduces a nearly consistent mass matrix. Part 2: Implementation', *Int. j. numer. methods fluids*, **11**, 621–659 (1990).
11. C. P. Jackson, 'A finite-element study of the onset of vortex shedding in flow past variously shaped bodies', *J. Fluid Mech.*, **182**, 23–45 (1987).
12. S. V. Patankar, *Numerical Heat Transfer and Fluid Flow*, Hemisphere/McGraw-Hill, New York, 1980.
13. S. C. Eisenstat, M. C. Gursky, M. H. Schultz and A. H. Sherman, 'The Yale Sparse Matrix Package, I. Symmetric problems, II. The nonsymmetric codes', *Research Reports 112 and 114*, Department of Computer Science, Yale University, 1977.
14. K. M. Kelkar, 'Numerical study of stability of fluid motion', *Ph.D. Thesis*, University of Minnesota, 1988.